Subcellular distribution of an inhalational anesthetic *in situ*

RODERIC G. ECKENHOFF AND HENRY SHUMAN

Department of Anesthesia, Institute for Environmental Medicine, and Pennsylvania Muscle Institute, University of Pennsylvania Medical Center, Philadelphia, PA 19104-6068

ABSTRACT To better understand the mechanisms and sites of anesthetic action, we determined the subcellular partitioning of halothane in a tissue model. A method was found to fix the *in vivo* distribution of halothane in rat atrial tissue for subsequent electron microscopy and x-ray microanalysis. Atrial strips were exposed to various concentrations of halothane, rapidly frozen, cryo-sectioned, and cryo-transferred into an electron microscope. Irradiation of the hydrated cryosections with the electron beam caused halothane radiolysis, which allowed retention of the halogen-containing fragments after dehydration of the sections. The bromine from halothane was detected and quantified with x-ray microanalysis in various microregions of atrial myocytes. Halothane (bromine) partitioned largely to mitochondria, with progressively lower concentrations in sarcolemma, nuclear membrane, cytoplasm, sarcomere, and nucleus. Partitioning could not be explained solely by distribution of cellular lipid, suggesting significant and differential physicochemical solubility in protein. However, we found no saturable compartment in atrial myocytes within the clinical concentration range, which implies little specific protein binding.

Because of the close correlation of potency with lipid solubility, inhalational anesthetics have been considered to act through perturbations of the lipid component of cellular membranes (1). Recent evidence, however, suggests that anesthetics may have direct interactions with cellular proteins that could be responsible for anesthetic action (2). An *in vivo* fluorine NMR study concluded that the majority of halothane in brain occupied a tightly bound environment that showed saturation within the clinical concentration range (3). Other investigators have demonstrated direct inhibition of an *in vitro* enzyme (4). Thus, if significant binding to cellular protein does exist, anesthetic partitioning on a subcellular level may not correlate with the distribution of cellular lipid or show simple physicochemical solubility characteristics. To evaluate subcellular partitioning of the popular inhalational anesthetic halothane, we developed a method for the fixation of a halogenated gas in tissue for subsequent microscopic localization and were able to measure halothane concentration with subcellular resolution.

METHODS

Animal protocols were approved by the Institutional Animal Care and Use Committee. Atrial tissue was chosen for study because of freezing quality, ease and tolerance of preparation, and the presence of a morphologically discrete contractile protein compartment (sarcomeres). Atrial strips were prepared from Sprague–Dawley rats after cervical dislocation. The strips were tied, endocardial surface up, over clean wooden pins under slight tension and incubated in 30°C Krebs–Ringer buffer at pH 7.40, equilibrated with 95% oxygen/5% carbon dioxide and 0, 1.5, or 4.7% halothane gas (by

Table 1. Hydrated/dehydrated bromine retention analysis in two experiments (4.7% halothane)

	Hydrated/dehydrated ratio	
Br	Br/P	Br/K
0.19 ± 0.03	1.21 ± 0.03	1.22 ± 0.08

X-ray spectra were collected from large (100 μm diameter) probes (average dose = 0.8 electron per Å^2) in the hydrated sections and in the same area after dehydration (areas included myocytes, connective tissue, and interstitial space). Ratios of hydrated/dehydrated bromine concentrations, as determined from peak to continuum ratio analysis, and the hydrated/dehydrated ratio of bromine to less-volatile elements, phosphorus and potassium, are shown.

gas chromatography). After 60 min, the atrial strips were rapidly frozen by plunging the pins into Freon 22 cooled to −165°C with liquid nitrogen. Thin cryosections ($\approx$150 nm) were prepared on a Reichert cryoultramicrotome and transferred at −150°C (Gatan cryotransfer stage) into a Philips 400T electron microscope equipped with a Si(Li) energy-dispersive x-ray detector and a Kevex 7000 multichannel analyzer interfaced to a VAX 11-750 computer. Elemental concentrations were determined from peak to continuum ratio analysis (5, 6) and expressed as mmol per kg dry mass units. Since the unfixed unstained frozen-hydrated sections had insufficient contrast to visualize structure, the sections were warmed slowly to −100°C from the transfer temperature of −150°C and dehydrated by sublimation in the microscope vacuum of 10^{-8} torr (1 torr = 133.3 Pa). Pilot studies determined that if the sections were dehydrated before exposure to an electron beam, bromine was not detected with x-ray microanalysis. However, if the sections were exposed to the electron beam while hydrated, bromine was readily detected after dehydration.

The degree of bromine retention after "fixation" with the electron beam and dehydration was evaluated by collecting x-ray spectra from large areas (100 μm in diameter) of hydrated sections at −150 to −160°C (Table 1). The sections were then warmed to −100°C, and x-ray spectra were again collected from the same area of the now dehydrated sections; bromine concentration was measured in both.

Electron beam-exposed dehydrated sections were warmed to 20°C, removed from the microscope, carbon-coated (3–5 nm), and reexamined with x-ray microanalysis for bromine partitioning between readily observable subcellular compartments (Fig. 1): perinuclear cytoplasm, sarcomere, nucleus, and mitochondria. In addition, spectra were collected from astigmatic line probes (1500–3000 × 20–30 nm) placed over sarcolemma and nuclear membrane, which are readily visualized in well frozen areas, even in unfixed unstained cryosections. Spectra from such "line" probes contain contributions from adjacent regions and thus are "membrane-enriched," rather than pure membrane spectra. Sarcoplasmic reticulum membranes could not be readily resolved from adjacent membrane structures.

Abbreviation: FCCP, carbonylcyanide *p*-trifluoromethoxyphenylhydrazone.

Medical Sciences: Eckenhoff and Shuman

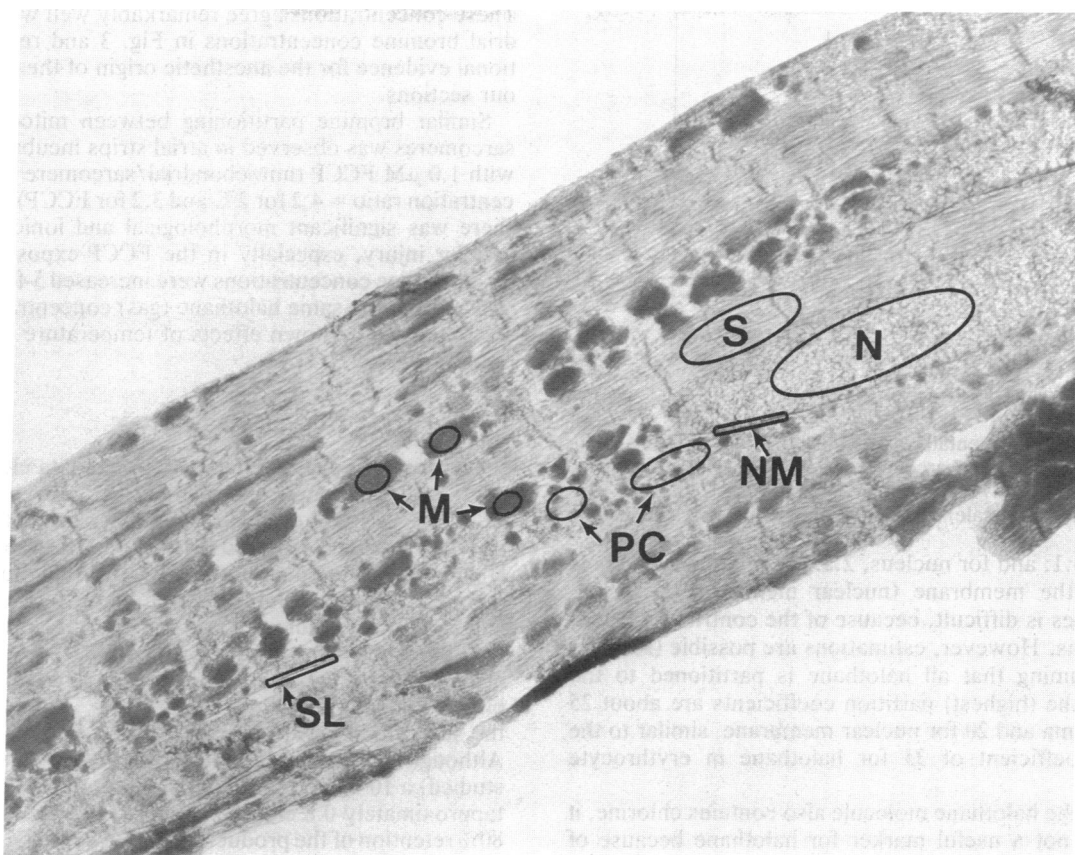*Proc. Natl. Acad. Sci. USA* 87 *(1990)* 455

Fig. 1. Electron micrograph of atrial cryosection after dehydration in the electron microscope. Representative probe areas are indicated by enclosed lines. S, sarcomere; N, nucleus; M, mitochondria; PC, perinuclear cytoplasm; NM, nuclear membrane; SL, sarcolemma.

To determine if metabolic activity was responsible for the observed partitioning, additional atrial strips were incubated at 2°C or with a protonophore mitochondrial uncoupler [1.0 μM carbonylcyanide p-trifluoromethoxyphenylhydrazone (FCCP) (7)] for the same period of time in 1.5% halothane and processed in the same way as above. Also, to assure that the measured halothane partitioning was representative of the *in vivo* state, cell integrity was evaluated simultaneously with measurement of bromine concentrations, using morphologic (cell or mitochondrial swelling, sarcomere disruption, and interstitial or intercalated disk widening) or ionic criteria (changes in the normally low sodium/potassium ratios or cytoplasmic/mitochondrial calcium concentrations).

RESULTS

There was no morphological or ionic evidence for cellular injury in the atrial myocytes exposed to halothane with the exception of those tissues exposed to cold or FCCP (see below).

Bromine fixation in cryosections exposed to an electron beam was evaluated by determining whole-cell bromine concentrations for four conditions: 0% halothane/no beam; 0% halothane/beam; 4.7% halothane/no beam; 4.7 halothane/beam (Table 2). Bromine was measurable only in sections that were exposed both to halothane and to the electron beam. Comparison of hydrated to dehydrated elemental concentrations allowed estimation of bromine retention after fixation and dehydration. The average bromine hydrated/dehydrated concentration ratio of about 0.2 (assuming 80% tissue hydration) and the hydrated/dehydrated ratio of bromine normalized to nonvolatile elements (phosphorus and potassium) of about 1.2 imply greater than 80% retention of the halothane-derived bromine after fixation and

dehydration. Also, the calculated partition coefficient for the whole cell (from Table 2) of 4.4, which agrees well with a reported value of 3.8 for skeletal muscle (8), is further evidence for retention.

The roughly linear relationship of all subcellular compartmental bromine concentrations with halothane gas concentration (0–4.7%) (Figs. 2 and 3) is evidence against a large concentration of specific saturable binding sites for the halothane molecule in atrial myocytes. The concentration data in Fig. 3 allow the calculation of *in situ* compartmental gas partition coefficients (8) (assuming hydration values for cytoplasm, nucleus, and sarcomere of 80%; and mitochondria of 60%): for mitochondria, 14.4; for cytoplasm, 4.0; for

Table 2. Whole atrial cell bromine concentration with and without radiolytic fixation

	Br concentration, mmol/kg (dry weight)		
Condition	0%	1.5%	4.7%
No-beam	1.7 ± 0.7 (15)	2.0 ± 1.4 (7)	0.1 ± 0.9 (9)
Beam	−0.3 ± 0.8 (15)	15.5 ± 3.0 (17)	40.3 ± 5.7 (20)

Data are mean ± SEM and numbers in parentheses are the number of cells in two experiments at halothane concentrations of 0%, 1.5%, and 4.7%. Beam grids were exposed to a low-current electron beam (100 pA) at 80 kV accelerating voltage for ≈10 min before dehydrating by warming to −100°C. Other grids were dehydrated without exposure to an electron beam (No-beam group). X-ray spectra were collected from multiple random probes over several compartments within many cells; bromine concentrations were determined and averaged to obtain whole-cell bromine concentrations. Since the bromine x-ray L-line (1.59 keV) overlaps the aluminum K-line (1.49 keV), the bromine concentrations for no-beam cells verifies the absence of aluminum contamination in these samples. The presence of bromine was further verified by detection of its K-line at 11.9 keV.
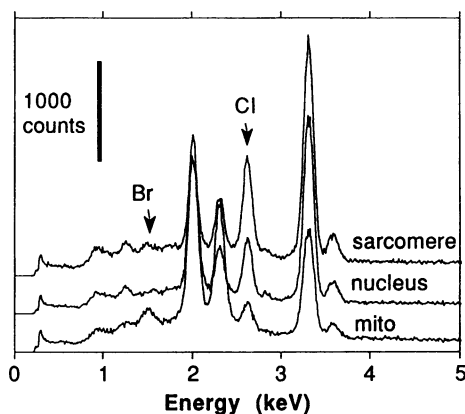
FIG. 2.   Three representative x-ray spectra from different compartments (mitochondria, sarcomere, and nucleus) in a rat atrial myocyte exposed to 4.7% halothane. The bromine L-line (Br) (the 11.9-keV K-line is off scale) and the chlorine K-line (Cl) are labeled.

sarcomere, 3.1; and for nucleus, 2.2. Calculating such coefficients for the membrane (nuclear membrane or sarcolemma) probes is difficult, because of the contribution from adjacent areas. However, estimations are possible (see Fig. 3) and, assuming that all halothane is partitioned to the membrane, the (highest) partition coefficients are about 25 for sarcolemma and 20 for nuclear membrane, similar to the measured coefficient of 35 for halothane in erythrocyte ghosts (9).

Although the halothane molecule also contains chlorine, it is generally not a useful marker for halothane because of endogenous levels of chlorine in mammalian tissues. However, because normal mitochondria have a low chlorine content (10), it was possible to measure the incremental increase in mitochondrial chlorine due to halothane and provide an additional test of halogen fixation. Thus, a mean mitochondrial chlorine excess of 27 mmol/kg (dry wt) at 1.5% and 71 mmol/kg (dry wt) at 4.7% halothane was found in sections that were fixed as compared to sections from the same tissue block that were dehydrated without fixation.
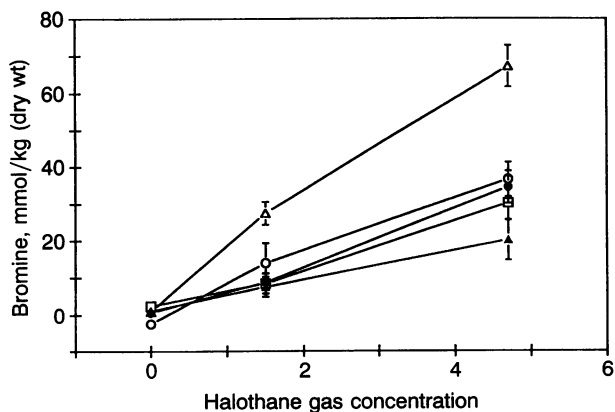

FIG. 3.   Subcellular compartmental bromine concentrations as related to gas concentration [% (vol/vol)] of halothane. Sections were handled as in Table 1, except that all were radiolysis-fixed. Cytoplasm (○) represents perinuclear cytoplasm including granules. Sarcomere (●), mitochondria (△), and nucleus (▲) represent probes entirely within the specified compartment. Sarcolemma (□) was a focused astigmatic line probe over this structure. Nuclear membrane is not shown on this figure; it was essentially the same as sarcolemma. Since the estimated width of these line probes and membrane was 30 and 8 nm, respectively, membrane constitutes about 30% of the line probe volume. However, since the hydration of adjacent areas is greater than membrane (80% vs. 10%), the mass of membrane in the line probe is about 50%.

These concentrations agree remarkably well with mitochondrial bromine concentrations in Fig. 3 and represent additional evidence for the anesthetic origin of these halogens in our sections.

Similar bromine partitioning between mitochondria and sarcomeres was observed in atrial strips incubated at 2°C or with 1.0 μM FCCP (mitochondrial/sarcomere bromine concentration ratio = 4.2 for 2°C and 3.2 for FCCP), even though there was significant morphological and ionic evidence of cellular injury, especially in the FCCP-exposed tissue. At 2°C, bromine concentrations were increased 5-fold over what was seen at the same halothane (gas) concentration at 30°C, consistent with known effects of temperature on anesthetic solubility (9).

DISCUSSION

Halothane Radiolytic Fixation. These data clearly demonstrate that the source of bromine in the cryosections was halothane and that electron beam exposure before warming and dehydration is required for bromine retention or fixation. High-energy electrons, photons, and γ-radiation have been reported to cause radiolysis of halothane to halogen ions and halocarbon free radicals (11), and it is likely that a similar reaction is occurring in our cryosections while exposed to the electron beam. These reactive halogenated species probably bind to nonvolatile cellular components, allowing retention in the section after warming and dehydration of our sections. Although the time requirement for these reactions was not studied, a 10-min exposure to a relatively low electron dose (approximately 0.8 electrons per Å^2) produced greater than 80% retention of the products of radiolysis. The fact that little bromine is lost from the section during radiolytic fixation (Table 2) is important since this also implies that the lateral diffusion of bromine from its original location (when frozen) is less than the 150-nm section thickness. The observation that chlorine and bromine are retained similarly suggests that the major halothane radiolysis products [bromine ion and 1-chloro-2,2,2-trifluoroethyl free radical (11)] both bind to nonvolatile cellular constituents. The low-energy fluorine x-ray was not detected due to absorption by the detector window.

Halogenated gas can be fixed in thin biological specimens and measured with electron microscopy and microanalysis. This technique measures gas distribution at an electron microscope level of resolution and raises the potential for extension to other gases.

Halothane Partitioning. Conventional views suggest that distribution of anesthetic in the lipid component of biological membranes is responsible for anesthetic action (1). However, lipid solubility alone does not explain the halothane (bromine) concentrations observed in the subcellular compartments in this study. For example, if halothane distributes into mitochondrial lipid alone (less than 10% of mitochondrial mass), the calculated lipid/gas partition coefficient would have to be greater than 350, severalfold higher than reported for lipid bilayers (9). The reported lipid bilayer/gas coefficient of 80 (at 30°C) (8, 9) implies that nonlipid mitochondrial components (largely protein) should have a coefficient of about 9, which is several times greater than the sarcomere or nuclear compartments (little lipid in either) or proteins such as albumin, globulin, or hemoglobin (12). This differential solubility in nonlipid cellular components implies some specificity and is consistent with recent studies that suggest a direct protein site of action for the inhalational anesthetics (2). A recent NMR study suggested that halothane occupies a saturable environment in brain (3), suggesting a highly specific binding site, and reported that this site accounted for approximately 80% of the brain halothane content. Although our technique may not detect saturation in a low-concen-

Medical Sciences: Eckenhoff and Shuman

Proc. Natl. Acad. Sci. USA 87 (1990)   457

tration compartmental protein, we certainly should have been able to detect a component of such proportions. Since bromine concentrations in all compartments showed linearity with respect to gas concentration (clinical range), the saturable sites or environments must either be specific to neuronal tissue or be an artifact of the *in vivo* fluorine NMR model (13).

The ineffectiveness of cold or an uncoupler on subcellular halothane partitioning indicates that maintenance of active transport and proton gradients is not necessary for the high mitochondrial halothane concentrations. The fact that halothane (bromine) concentrations are 5 times higher under cold (2°C) as opposed to warm (30°C) conditions reinforces the physicochemical nature of halothane's subcellular partitioning. The presence of high halothane concentrations in mitochondria does not necessarily indicate a mitochondrial site for production of anesthesia. It is consistent, however, with reported effects of halothane on mitochondrial membranes and metabolism (14, 15).

In summary, halothane subcellular partitioning appears to be physicochemical, and, although the data suggest substantial and differential solubility in protein, no saturable compartments were observed in the clinical concentration range. We emphasize that this steady-state subcellular halothane partitioning cannot yet be related to anesthetic action, but integration of this technique with both kinetic and functional indices may provide important clues to the site and mechanism of anesthetic action.

1. Albrecht, R. R. & Miletich, D. J. (1988) *Gen. Pharmacol.* **19**, 339–346.
2. Franks, N. P. & Lieb, W. R. (1982) *Nature (London)* **300**, 487–493.
3. Evers, A. S., Berkowitz, B. A. & d'Avignon, D. A. (1987) *Nature (London)* **328**, 157–160.
4. Franks, N. P. & Lieb, W. R. (1986) *Proc. Natl. Acad. Sci. USA* **83**, 5116–5120.
5. Shuman, H., Somlyo, A. V. & Somlyo, A. P. (1976) *Ultramicroscopy* **1**, 317–339.
6. Kitazawa, T., Shuman, H. & Somlyo, A. P. (1983) *Ultramicroscopy* **11**, 251–262.
7. Veit, P., Fuchs, J. & Zimmer, G. (1985) *Basic Res. Cardiol.* **80**, 107–115.
8. Eger, E. I. (1974) *Anesthetic Uptake and Action* (Williams & Wilkins, Baltimore).
9. Smith, R. A., Porter, E. A. & Miller, K. (1981) *Biochim. Biophys. Acta* **645**, 327–338.
10. Somlyo, A. P., Bond, M. & Somlyo, A. V. (1985) *Nature (London)* **314**, 622–625.
11. Lal, M., Schoneich, C., Monig, J. & Asmus, K. D. (1988) *Int. J. Radiat. Biol.* **54**, 773–785.
12. Laasberg, L. H. & Hedley-White, J. (1970) *Anesthesiology* **32**, 351–356.
13. Franks, N. P. (1987) *Nature (London)* **328**, 113.
14. Rottenberg, H. (1983) *Proc. Natl. Acad. Sci. USA* **80**, 3313–3317.
15. Romero, F. J., Pallardo, F. V., Bolinches, R., Roma, J., Saez, G. T., Noli, T. & deGroot, H. (1987) *J. Appl. Physiol.* **63**, 1776–1780.